Published in final edited form as:
Gene. 1999 June 11; 233(1-2): 39–47.

Characterization of the components of the putative mammalian sister chromatid cohesion complex

N. Darwiche[1,2], **L.A. Freeman**[2], and **A. Strunnikov**[*]
Unit of Chromosome Structure and Function, NIH, NICHD, Laboratory of Molecular Embryology, 18T Library Drive, room 106, Bethesda, MD 20892-5430, USA

Abstract

Establishing and maintaining proper sister chromatid cohesion throughout the cell cycle are essential for maintaining genome integrity. To understand how sister chromatid cohesion occurs in mammals, we have cloned and characterized mouse orthologs of proteins known to be involved in sister chromatid cohesion in other organisms. The cDNAs for the mouse orthologs of *SMC1*$^{S.c.}$ and *SMC3*$^{S.c.}$, *mSMCB* and *mSMCD* respectively, were cloned and the corresponding transcripts and proteins were characterized. *mSMCB* and *mSMCD* are transcribed at similar levels in adult mouse tissues except in testis, which has an excess of *mSMCD* transcripts. The mSMCB and mSMCD proteins, as well as the PW29 protein, a mouse homolog of Mcd1p$^{S.c.}$/Rad21$^{S.p.}$, form a complex similar to cohesin in *X. laevis*. mSMCB, mSMCD and PW29 protein levels show no significant cell-cycle dependence. The bulk of the mSMCB, mSMCD and PW29 proteins undergo redistribution from the chromosome vicinity to the cytoplasm during prometaphase and back to the chromatin in telophase. This pattern of intracellular localization suggests a complex role for this group of SMC proteins in chromosome dynamics. The PW29 protein and PCNA, which have both been implicated in sister chromatid cohesion, do not colocalize, indicating that these proteins may not function in the same cohesion pathway. Overexpression of a PW29-GFP fusion protein in mouse fibroblasts leads to inhibition of proliferation, implicating this protein and its complex with SMC proteins in the control of mitotic cycle progression.

Keywords

Cell cycle; Chromosome; PW29; SMC proteins

1. Introduction

Sister chromatid cohesion is essential for proper chromosome segregation during cell division. Sister chromatid cohesion is established during S phase and is maintained until the metaphase-to-anaphase transition. As long as cohesion is properly established and maintained, the kinetochore of each sister chromatid will capture microtubules from opposite spindle poles, and each daughter cell will therefore receive one chromosome. However, if sister chromatid cohesion is not established or is not maintained, then two sister kinetochores might attach to microtubules from the same spindle pole. In this case, one daughter cell would receive two sister chromatids, and the other daughter would receive none. Thus, sister chromatid cohesion is important for accurate transmission of the genetic material.

*Corresponding author. Tel.: +1-301-402-8384; fax: +1-301-402-1323. E-mail address: E-mail: strunnik@box-s.nih.gov (A. Strunnikov).
[1]Present address: American University of Beirut, Biochemistry and Biology Department, DTS4-44, 850 Third Avenue, New York, NY 10022-6222, USA.
[2]These two authors contributed equally to this work.

Recent work has identified a number of proteins involved in establishing and maintaining sister chromatid cohesion (Biggins and Murray, 1998). The *S. cerevisiae* proteins Smc1p, Smc3p and Mcd1p (also known as Scc1p) have well-established roles in sister chromatid cohesion (Michaelis et al., 1997; Strunnikov, 1998). The *X. laevis* homologs of these proteins, termed XSMC1, XSMC3 and XRAD21, along with two other proteins, are all components of a complex that promotes sister chromatid cohesion in vitro (Losada et al., 1998). This complex is termed the 'cohesin' complex. Interestingly, the mammalian multiprotein recombination complex RC-1 is able to catalyze renaturation of single-stranded DNA, and includes bovine homologs of XSMC1 and XSMC3 (Jessberger et al., 1996; Stursberg et al., 1999). Homologs of *SMC1* and *SMC3*, *hSMC1* and *hSMC3*, have also been identified in humans (Schmiesing et al., 1998).

As a part of the ongoing effort to identify and characterize the components of the sister chromatid cohesion machinery in mammals, we report here the isolation of cDNA clones for the mouse orthologs of *SMC1* and *SMC3*, termed, respectively, *mSMCB* and *mSMCD* and characterization of the PW29 protein, an ortholog of Mcd1p. We have characterized the expression pattern and intracellular localization of these putative sister chromatid cohesion proteins throughout the cell cycle. *M. musculus* is an excellent system for direct visualization of chromosomes and offers the possibility of genetic and developmental studies. Future work with this system should considerably enhance our understanding of sister chromatid cohesion and maintenance of genome integrity in mammalian cells.

2. Materials and methods

2.1. Cloning and DNA sequencing

mSMCB was cloned in three steps. First, a 1.5-kb *Sal*I–*Eag*I fragment corresponding to the 5′-terminus of human *SB1.8* (Rocques et al., 1995) was used to screen a 7-day mouse embryo 5′-Stretch Plus lambda gt10 library (Clontech) by hybridization. Out of 57 positive clones, six types of inserts were subcloned into pBluescript II, partially sequenced and found to be overlapping. The plasmid (pND559) containing the longest *Eco*RI fragment (2.0 kb) was chosen for further analysis. This clone contained the 5′-half of the *mSMCB* coding sequence. The 3′ end of the cDNA was found in two EST clones, 670734 and 679754 (ATCC). The 5′ and 3′-terminal clones were joined by a 1.6-kb PCR fragment generated with Pfu polymerase (Stratagene) using mouse cDNA (Clontech) as a template.

mSMCD cDNA was cloned using a similar strategy. First, a human EST 134462 (ATCC) was used to screen lambda gt10 mouse 7-day embryo cDNA library (Clontech) by hybridization. Among 19 positive clones, four types of inserts were identified, subcloned into pBluescript II, partially sequenced and found to be overlapping. The longest (2 kb) clone pND562 contained the 3′ end of mSMCD cDNA. The 5′ end of mSMCD cDNA was found in mouse EST 603613 (ATCC). The two fragments were joined by creating a 0.8-kb PCR fragment generated with Pfu polymerase (Stratagene) from mouse cDNA template (Clontech).

A partial PW29 cDNA clone (*Eco*RI fragment) was obtained from T. Muramatsu (Yu et al., 1995). The 5′ end of the PW29 clone was cloned by PCR, using RACE-ready cDNA from Clontech. The full-length PW29 clone (*Sal*I–*Bgl*II) was assembled and cloned into the *Xho*I and *Bam*HI sites of pEGFP-N1 (Clontech) giving pND571 plasmid.

Template DNA was sequenced using the ABI Prism 377 sequencer (Perkin Elmer) and the dye-terminator method, with custom primers (Life Technologies). A sequence analysis was performed using AssemblyLign software (Eastman Kodak).

2.2. Cell culture and cell-cycle methods

Swiss mouse NIH3T3 fibroblasts (ATCC) were routinely maintained in Dulbecco's modified Eagle's medium (DMEM) (with high glucose, glutamine and sodium pyruvate), supplemented with 10% calf serum (CS), 100 μg/ml of penicillin and 100 μg/ml of streptomycin (all from Life Technologies), under 5%CO_2 in a humidified incubator (37°C). For cell-cycle studies, the NIH3T3 cells were arrested in G0 phase using serum starvation. Cells were washed once with DMEM medium (Life Technologies) without FBS, then fresh medium containing 0.5% FBS was added, and incubation was continued for 16–24 h. A G1-arrested population of NIH3T3 cells was obtained using treatment with lovastatin (Merck) (Reed et al., 1994). The NIH3T3 cells were treated upon reaching 30% confluence by adding lovastatin from a 4 mg/ml of stock solution to 8 μg/ml of final concentration, directly to the media. The cells were analyzed/harvested after 36 h. Synchronization in S-phase was achieved by arresting with aphidicolin (Sigma) similarly to lovastatin treatment. Aphidicolin was added to a final concentration of 1.3 μg/ml, and the cells were incubated for 16–19 h. A mitotic population of NIH3T3 cells was obtained by nocodazole treatment. First, nocodazole (0.7 μg/ml final) was added with fresh DMEM media to the 50%-confluent cells. After 16–19 h, mitotic cells were washed off without trypsinization. The specificity and degree of cell-cycle arrest using different treatments was monitored by FACScan (Becton Dickinson) according to the manufacturer's recommendations for propidium-iodide stained cells. Total protein was extracted from washed cells using lysis with 1% SDS. The protein concentration was determined using a protein assay from Pierce and SpectraMax340 reader (Molecular Devices).

To generate transfected cell lines expressing the PW29-GFP fusion, the population of NIH3T3 cells was transfected with the pND571 plasmid using the lipofectamine protocol (Life Technologies). The same protocol was used for control plasmids pEGFP-N1 (Clontech) and BOSH2BGFP-N1 (Kanda et al., 1998).

2.3. Antibodies

Antibodies against mSMCB were generated against the antigen expressed in BL21(DE3) pLysS strain of *E. coli* (Novagen). The antigen-producing construct was derived from human SB1.8 cDNA (Rocques et al., 1995). An *Xho*I-digested PCR fragment corresponding to the last 660 amino acid residues of the SB1.8 gene was cloned into the *Xho*I site of pRSETA (Invitrogen) in order to express a 76-kDa *SB1.8* fragment. The recombinant polypeptide (#550) encoded by this construct differs in only four amino acid positions from the mouse SMCB sequence. The antigen was purified sequentially by IMAC (ProBond, Invitrogen) and PAGE and then injected into two NZW rabbits (Covance). Production sera were affinity-purified on CNBr sepharose columns (Pharmacia) with the coupled purified recombinant protein and used in 1:500 dilution for Western blots and 1:2000 for immunofluorescence.

Anti-mSMCD antibodies were generated against the MAP-peptide (Research Genetics) PAPFYLFDEIDQALDAQHRKAVS inferred from mSMCD cDNA sequence. Production sera were affinity-purified on CNBr sepharose columns (Pharmacia) with the coupled purified recombinant protein #564 containing the corresponding peptide sequence as a part of a longer polypeptide. The corresponding expression plasmid pND564 was constructed by ligating a 2-kb *Eco*RI fragment of mSMCD cDNA into pRSETA (Invitrogen). The affinity-purified anti-mSMCD antibodies were used in a 1:250 dilution for Western blots and 1:1000 for immunofluorescence.

Anti-tubulin antibody YOL1/34 was from Harlan. Antibody against rabbit GA3PDH was from Biogenesis. All commercially available antibodies were used according to the manufacturer's recommendations. Anti-PW29 antibodies (Yu et al., 1995) were used in a 1:10 000 dilution for all experiments. The immunofluorescent staining of mouse NIH3T3 cells and Western blots

were performed according to standard protocols (Harlow and Lane, 1988; Pagano, 1995). Cells were fixed either in 4% paraformaldehyde in PBS for 5 min at room temperature or in cold methanol for 10 min. No detergent was used in washing steps or antibody dilution buffers. The results of two fixation protocols were found to be identical regarding mSMCB, mSMCD and PW29. Staining with preimmune sera corresponding to mSMCB or mSMCD did not yield any specific staining in Western blots or by indirect immunofluorescence.

Immunoprecipitations were performed using a mouse embryo extract. Usually, an equivalent of two 14-day embryos of 129cv mouse was used for one immunoprecipitation reaction. Extracts were routinely prepared from ten 14-day embryos and stored at −80°C. After homogenization (tissue homogenizer and sonication) in the extraction buffer EB (100 mM KCl, 50 mM HEPES-KOH, pH 7.5, 2.5 mM $MgCl_2$, 50 mM NaF, 5 mM Triton X100) (Liang and Stillman, $Na_4P_2O_7$, 0.25% 1997) and two centrifugations at 20 000×*g* (4°C) extracts were preincubated for 6 h at 4°C with protein A-sepharose beads (Pharmacia). After removal of the protein, A-sepharose extracts were centrifuged for 1 h at 40 000×*g*, and the supernatant was used for the immunoprecipitation reaction. Affinity-purified anti-mSMCB antibodies were cross-linked to CNBr-activated CL4-B sepharose and 50 μl of sepharose beads prepared in this way were used to immunoprecipitate proteins from 2 ml of extract. CL4-B beads without cross-linked antibody were used for mock immunoprecipitation.

2.4. Microscopy

Microscopy was performed with a wide-field Zeiss AxioVert microscope with epifluorescence. The images were collected using a MicroMax cooled CCD camera (Princeton Instruments) and a Z-axis motor assembly (Ludl). Eight to ten optical sections spanning 5 μm were collected for each field. Optical sections were converted into a stacked image with IP-Lab software (Scanalytics). For time-lapse microscopy, transfections were performed on the coverslip-glass Nunc chambers, allowing direct observation of the transfected cells with a conventional inverted microscope. The microscope stage was continuously heated to 37°C with a uniform air flow.

3. Results

3.1. Isolation and primary characterization of mSMCB and mSMCD cDNA clones and characterization of their expression

To initiate structure–function studies on the mouse sister chromatid cohesion complex, we cloned the cDNAs for *mSMCB* and *mSMCD*. The cDNA clones were isolated by a combination of screening a mouse embryonic cDNA library and of available EST clones (see Section 2). The *mSMCB* cDNA was found to encode a 1233-amino acid residue protein, whereas the *mSMCD* cDNA encodes a 1217-residue protein (Fig. 1). All signature motifs of the SMC family, i.e. the NTP-binding domain, the coiled-coil region and the DA-box, can be readily identified in both proteins. A comparative sequence analysis revealed that *mSMCB* and *mSMCD* are indeed the orthologs of *SMC1* and *SMC3*, respectively (Fig. 2). mRNA for both mSMCB (4.3 kb) and mSMCD (4.2 kb) were expressed in all adult mouse tissues tested (Fig. 3). Transcript levels for these genes were correlated to each other in all somatic tissues. These transcription profiles also corresponded to the reported profile of PW29 transcription. Interestingly, in mouse testis, a significant difference in mRNA level between mSMCB and mSMCD was found. This finding suggests that in the germline, the activity of these proteins may be regulated through expression of mSMCB. Alternatively, mSMCB and mSMCD may have some independent roles.

3.2. mSMCB, mSMCD and PW29 form a complex in the mouse embryo

Recent work has shown that in budding yeast, Mcd1p is associated with Smc1p when overexpressed (Guacci et al., 1997). A similar substoichiometric association between the corresponding proteins XRAD21 and XSMC1, as well as with XSMC3, has been also been reported for the cohesin protein complex purified from *X. laevis* egg extracts (Losada et al., 1998). We have begun to investigate the relationship between these proteins in mammalian cells. We generated rabbit polyclonal antibodies against the C-terminal region of mSMCB and used them for immunoprecipitation experiments with mouse embryonic extracts (Fig. 4). Antibodies against PW29 (Yu et al., 1995) and mSMCD (see Section 2) were used to monitor the corresponding proteins. mSMCB, mSMCD and PW29 are abundantly expressed in early mouse embryos, at both the mRNA and protein level of analysis (data not shown), possibly correlating with a high level of cell proliferation. We used mouse embryonic extracts for immunoprecipitation with antibodies against mSMCB. Analysis of the immunoprecipitates demonstrated that antibodies against mSMCB readily coimmunoprecipitate the mSMCD protein (Fig. 4). A band corresponding to the PW29 molecular weight was present in the same fraction. Since the PW29 protein is the only known Mcd1p homolog from mouse (Yu et al., 1995), this result suggests that in the somatic cells of mouse embryo, a complex exists, including mSMCB, mSMCD and PW29 proteins, analogous to the complex found in *S. cerevisiae* and in *X. laevis* eggs. This complex may thus be involved in chromosome structure maintenance and sister chromatid cohesion in mammalian cells.

3.3. Expression and intracellular localization of the mSMCB, mSMCD and PW29 proteins during the mitotic cell cycle

In budding yeast, the pattern of Mcd1p expression throughout the cell cycle differs from that of Smc1p and Smc3p (Guacci et al., 1997) (L.F. and A.S., unpublished). In addition, the Mcd1 protein leaves chromosomes during anaphase in budding yeast, while Smc proteins remain associated with chromatin (Guacci et al., 1997; Michaelis et al., 1997). These observations suggest that in budding yeast, the composition of the cohesin complex varies throughout the cell cycle.

To investigate the expression pattern of mSMCB, mSMCD and PW29 in mammalian cells, we monitored expression level of these proteins in cells arrested at different stages of the cell cycle (Fig. 5). NIH3T3 cells were arrested in the G1, G0, S and M phases by treatment with lovastatin, low serum concentration, aphidicolin and nocodazole, respectively (Fig. 5A). The expression of SMC proteins and PW29 was monitored by Western blotting. Both mSMCB and mSMCD proteins were expressed throughout the cell cycle in these cells (Fig. 5B), indicating that these proteins are not regulated throughout the cell cycle by changes in their expression level, similar to Smc1p and Smc3p expression in budding yeast. Antibodies against the PW29 protein also did not reveal any significant changes in the corresponding protein level throughout the cell cycle (Fig. 5B). This differs from the expression pattern displayed by Mcd1p in *S. cerevisiae* (Guacci et al., 1997;Michaelis et al., 1997), which is cell-cycle-dependent. Thus, regulation of PW29 in mouse fibroblasts differs from regulation of Mcd1p in *S. cerevisiae*. The activity of the PW29 protein in mammalian cells is most likely regulated at the posttranslational level.

We also investigated intracellular localization and cell-cycle regulation of the corresponding mouse proteins mSMCB, mSMCD and PW29. Since little is known about the specific regulatory mechanisms controlling mouse SMC proteins, these experiments were also designed to reveal whether these proteins change their localization during the cell cycle. Specific antibodies against mSMCB, mSMCD and PW29 were used to visualize these proteins in NIH3T3 cells using indirect immunofluorescence. Two alternative fixation methods were used in immunofluorescent staining (see Section 2). In all cases, specific antibodies for mSMCB,

mSMCD and PW29 proteins revealed a striking cell-cycle-dependent localization pattern (Fig. 6). The observed staining was consistent with the redistribution of these three proteins from the nucleus and chromosomes to the whole cell volume in prometaphase. The bulk of the mSMCB, mSMCD and PW29 proteins remained off the chromosomes throughout metaphase and anaphase. The chromosomal staining reappeared again in telophase (Fig. 6D; shown for PW29). Thus, the mSMCB, mSMCD and PW29 proteins displayed an almost identical intracellular localization relative to the chromosomes throughout all stages of the cell cycle examined, supporting the immunoprecipitation data suggesting that they form a complex. The mode of their intracellular redistribution during mitosis was also analogous to the data obtained for overexpressed Mcd1p in budding yeast (Guacci et al., 1997). The relative abundance of the PW29 protein in mitosis was, however, in sharp contrast to mitosis in budding yeast where Mcd1p is significantly downregulated (Guacci et al., 1997;Michaelis et al., 1997).

We have also obtained some evidence of selective chromatin binding of PW29 in mammalian cells (Fig. 7). We used PCNA, a DNA replication processivity factor, as a marker. Upon progression of S-phase most of the PCNA pool changes its localization from bulk chromatin to the nucleoli and from euchromatin to heterochromatin (Kelman, 1997). Double immunofluorescent staining of an asynchronous population of NIH3T3 cells demonstrated that pW29 does not relocate with PCNA (Fig. 7), suggesting that it, and probably the whole complex, has a specific chromatin-binding preference. Such preference may be limited either by local chromatin structure, by the timing of chromatin replication or by some specific sites where sister chomatid cohesion occurs.

3.4. Overexpression of PW29 causes arrest of cell division

The localization pattern of mSMCB, mSMCD and PW29 during metaphase suggests that the corresponding complex leaves chromosomes at the prometaphase–metaphase transition. Such precise timing of release of the complex from chromatin must be under thorough regulatory control by the cell-cycle machinery. Thus, overexpression of one of the components of the complex may unbalance this control and cause chromosomal aberrations throughout the cell cycle. In budding yeast, overexpression of Smc1p, Smc3p or Mcd1p does not result in any detectable phenotypic changes. However, mammalian chromosomes are substantially more complex and may respond to such an imbalance.

We overexpressed the PW29-GFP protein in NIH3T3 cells and applied selection for the G418 resistance marker. Whereas expression of the chimera was evident during the first 24 h after transfection, it disappeared after 72 h of G418-selection (data not shown) when the whole transfected population was analyzed. Also, of 20 randomly selected G418-resistant stable transfectants, none had any detectable expression of the PW29-GFP fusion protein. This effect was not due to the toxicity of the GFP molecule itself since, in control experiments with expression of GFP alone (which was partially localized in the nucleus) or expression of H2B-GFP (nuclear localization) (Kanda et al., 1998), no toxicity was detected. To investigate this phenomenon in more detail, we followed the fate of cells overexpressing PW29-GFP using real-time microscopy. Cells originally in interphase did not enter mitosis (eight cells monitored) and cells originally in mitosis never initiated anaphase (two cells monitored) over a 12-h observation period beginning 16 h after transfection. This observation suggests that the overexpression of PW29-GFP is disruptive to cell progression through the mitotic cell cycle. The nature of this inhibition and its possible mechanisms are to be investigated with regulated conditional expression of PW29 and site-specific mutants.

4. Discussion

We have cloned and sequenced the *mSMCB* and *mSMCD* cDNAs from *M. musculus*. The corresponding genes are orthologs of the *SMC1* and *SMC3* genes, which are known components

of the sister cohesion complex in *S. cerevisiae* and *X. laevis* (Guacci et al., 1997; Michaelis et al., 1997; Losada et al., 1998). The mSMCB and mSMCD proteins coimmunoprecipitate with each other and with the PW29 protein. PW29 is homologous to Mcd1p and to XRAD21, components of the sister chromatid cohesion complexes in *S. cerevisiae* and *X. laevis*, respectively. Thus, the mSMCB-mSMCD-PW29 complex that we have characterized from mouse embryo extract is most likely the mouse sister chromatid cohesion complex. Further analysis of the complex will elucidate its exact molecular function in mammalian cells.

Transcript levels for mSMCB and mSMCD show covariance in different tissues, further supporting the hypothesis that these two proteins form a complex. The only exception is testis, in which levels of mSMCD transcripts exceed levels of mSMCB transcripts. It will be interesting to determine whether testis contains a specialized SMC variant that substitutes for the lowered levels of mSMCB, and/or whether an imbalance of SMC proteins in testis plays a physiological role, or whether in this tissue mSMCB and mSMCD play independent roles.

To gain some insight into the mechanism of action of these proteins, we have examined their expression and localization throughout the cell cycle. The levels of the three proteins mSMCB, mSMCD and PW29 do not vary throughout the cell cycle. The intracellular localization, however, does. During interphase, immunofluorescent staining reveals that mSMCB, mSMCD and PW29 all localize to the nucleus and chromosomal region. At prometaphase, these three proteins redistribute mostly to the whole cell volume and remain mostly off the chromosomes throughout metaphase and anaphase, relocalizing to the chromosomes at telophase. This behavior is not what might be expected from a sister chromatid cohesion complex. Sister chromatid cohesion is established during DNA replication and persists until metaphase, yet the bulk of the mSMCB-mSMCD-PW29 complex exits the chromosomes before metaphase. It is possible that a small fraction of the complex, below the limit of sensitivity of the immunofluorescence technique, does remain associated with chromosomes throughout mitosis. Perhaps this fraction is responsible for maintaining cohesion until the metaphase–anaphase transition, and the bulk that is removed plays some interphase-specific role in chromosome function and must be removed to facilitate the dissolution of cohesion at metaphase. An alternative explanation for the disappearance of most of the mSMCB-mSMCD-PW29 complex from chromosomes during mitosis is that the complex may be involved only in establishment of cohesion and not maintenance (again perhaps playing other roles throughout the cell cycle). Similar behavior has been observed for hSMC1 (Schmiesing et al., 1998) and XSMC3 (Losada et al., 1998). In our study, the proteins visualized by immunofluorescence are endogenous proteins, and the results are therefore not artefacts of transfection or overexpression.

The behavior of the mSMCB-mSMCD-PW29 complex in mouse throughout the cell cycle does not precisely parallel that of the Smc1p–Smc3–Mcd1p complex in yeast. Nonetheless, it seems possible that the two complexes accomplish similar functions but in slightly different fashions. Levels of yeast Smc1p and Smc3p, like their mouse homologs mSMCB and mSMCD, do not vary throughout the cell cycle (L.F. and A.S., unpublished observations). Yeast Mcd1p localizes to the nucleus (Guacci et al., 1997) and particularly to chromatin (Uhlmann and Nasmyth, 1998) in S phase and more weakly to the nucleus at M phase. Similarly, mouse PW29 localizes strongly to the chromosomal region in interphase and only slightly to the chromosomal region in mitosis. Thus, in both yeast and mouse, levels of chromosomal Mcd1p and PW29, respectively, are high at S phase but significantly lower at metaphase. *S. cerevisiae* appears to accomplish this by regulating levels of Mcd1p transcript and protein, whereas *M. musculus* does not vary its levels of PW29 and thus must downregulate chromosomal levels of PW29 by alternative means, probably posttranslational modifications or interaction with regulatory factors. In both cases, the end result appears to be high levels of Mcd1p/PW29 in the chromatin region during S phase, and lower (but detectable) levels still

present at mitosis. It will be of interest to determine the mechanisms ensuring that this key member of the sister chromatid cohesion complex behaves in this conserved manner.

One of the unexpected results of our study was that mouse PW29, and probably the whole putative cohesin complex in mouse cell, does not colocalize with PCNA. PCNA has been linked to the recently identified *S. cerevisiae* cohesion factor Ctf7p, whose mechanistic role in cohesion has not yet been established. A temperature-sensitive mutation in yeast *CTF7* is suppressed by the yeast gene for PCNA, *POL30* (Skibbens et al., 1999). The PCNA and Ctf7 proteins are conserved between mouse and budding yeast. If a hypothetical PCNA/Ctf7p complex is involved in loading 'chromatid glue' onto DNA after chromatin replication as proposed (Skibbens et al., 1999), one might expect PW29 and PCNA to exhibit similar localization patterns. The fact that they do not fully colocalize in mouse cells may indicate that the PCNA/Ctf7 pathway is independent of the mSMCB–mSMCD–PW29 pathway. There is also a possibility that the mSMCB–mSMCD–PW29-based complex is involved in a process other than sister chromatid cohesion since no functional studies of its role in mammals have been carried out. There is, however, an indication that the SMC components of this complex are shared with the RC1 complex, involved in genetic recombination (Stursberg et al., 1999).

We found that overexpression of PW29-GFP appears to prevent progression of the cell cycle. The mechanism of this inhibition is unknown. SMC proteins are stably and stoichiometrically associated with each other (Hirano, 1998; Schmiesing et al., 1998). However, the Mcd1p, XRAD21 and probably PW29 proteins are associated with the corresponding SMC heterodimer less stably and in substoichiometric ratio and, for Mcd1p at least, in a cell-cycle-dependent fashion (Guacci et al., 1997; Losada et al., 1998). Thus, an imbalance in PW29 expression may potentially have negative implications for the activity of the cohesion complex in eukaryotic cells. This result may lead to a simple assay system to identify the functionally significant domains of the PW29 protein.

Acknowledgements

We thank S. Yu and T. Muramatsu for research materials, J. Lippincott-Schwartz for comments on the manuscript, J. Stroboulis and K. Wassarman for technical advice and M. Patente for technical help. N.D. and L.F. were recipients of a NICHD Intramural Research Training Award.

Abbreviations

bp
: base pair(s)

cDNA
: complementary DNA

EST
: expressed sequence tag

kb
: 1000 bp

References

Biggins S, Murray AW. Sister chromatid cohesion in mitosis. Curr Opin Cell Biol 1998;10:769–775. [PubMed: 9914173]

Guacci V, Koshland D, Strunnikov A. A direct link between sister chromatid cohesion and chromosome condensation revealed through the analysis of MCD1 in *S. cerevisiae* [see comments]. Cell 1997;91:47–57. [PubMed: 9335334]

Harlow, E.; Lane, D. Antibodies: a Laboratory Manual. Cold Spring Harbor Laboratory Press; Cold Spring Harbor, NY: 1988.

Hirano T. SMC protein complexes and higher-order chromosome dynamics. Curr Opin Cell Biol 1998;10:317–322. [PubMed: 9640531]

Jessberger R, Riwar B, Baechtold H, Akhmedov A. SMC proteins constitute two subunits of the mammalian recombination complex RC-1. EMBO J 1996;15:4061–4068. [PubMed: 8670910]

Kanda T, Sullivan KF, Wahl GM. Histone-GFP fusion protein enables sensitive analysis of chromosome dynamics in living mammalian cells. Curr Biol 1998;8:377–385. [PubMed: 9545195]

Kelman Z. PCNA: structure, functions and interactions. Oncogene 1997;14:629–640. [PubMed: 9038370]

Liang C, Stillman B. Persistent initiation of DNA replication and chromatin-bound MCM proteins during the cell cycle in *cdc6* mutants. Genes Dev 1997;11:3375–3386. [PubMed: 9407030]

Losada A, Hirano M, Hirano T. Identification of *Xenopus* SMC protein complexes required for sister chromatid cohesion. Genes Dev 1998;12:1986–1997. [PubMed: 9649503]

Michaelis C, Ciosk R, Nasmyth K. Cohesins: chromosomal proteins that prevent premature separation of sister chromatids. Cell 1997;91:35–45. [PubMed: 9335333]

Pagano, M. Cell Cycle — Materials and Methods. Springer; New York: 1995.

Reed SI, Bailly E, Dulic V, Hengst L, Resnitzky D, Slingerland J. G1 control in mammalian cells. J Cell Sci 1994;18(Suppl):69–73.

Rocques P, Clark J, Ball S, Crew J, Gill S, Christodoulou Z, Borts R, Louis E, Davies K, Cooper C. The human SB1.8 gene (DXS423E) encodes a putative chromosome segregation protein conserved in lower eukaryotes and prokaryotes. Hum Mol Genet 1995;4:243–249. [PubMed: 7757074]

Schmiesing JA, Ball AR Jr, Gregson HC, Alderton JM, Zhou S, Yokomori K. Identification of two distinct human SMC protein complexes involved in mitotic chromosome dynamics. Proc Natl Acad Sci USA 1998;95:12906–12911. [PubMed: 9789013]

Skibbens RV, Corson LB, Koshland D, Hieter P. Ctf7p is essential for sister chromatid cohesion and links mitotic chromosome structure to the DNA replication machinery. Genes Dev 1999;13:307–319. [PubMed: 9990855]

Strunnikov AV. SMC proteins and chromosome structure. Trends Cell Biol 1998;8:454–459. [PubMed: 9854313]

Stursberg S, Riwar B, Jessberger R. Cloning and characterization of mammalian SMC1 and SMC3 genes and proteins components of the DNA recombination complexes RC-1. Gene 1999;228:1–12. [PubMed: 10072753]

Uhlmann F, Nasmyth K. Cohesion between sister chromatids must be established during DNA replication. Curr Biol 1998;8:1095–1101. [PubMed: 9778527]

Yu S, Ozawa M, Naved AF, Miyauchi T, Muramatsu H, Muramatsu T. cDNA cloning and sequence analysis of a novel calcium binding protein with oligoproline motif. Cell Struct Funct 1995;20:263–268. [PubMed: 8521526]

mSMCB

MGFLKLIEIE NFKSYKGRQI IGPFQRFTAI IGPNGSGKSN LMDAISFVLG EKTSNLRVKT
LRDLIHGAPV GKPAANRAFV SMVYSEEGAE DRTFARVIVG GSSEYKINNK VVQLHEYSEE
LEKLGILIKA RNFLVFQGAV ESIAMKNPKE RTALFEEISR SGELAQEYDK RKKEMVKAEE
DTQFNYHRKK NIAAERKEAK QEKEEADRYQ RLKDEVVRAQ VQLQLFKLYH NEVEIEKLNK
ELASKNKEIE KDKKRMDKVE DELKEKKKEL GKMMREQQQI EKEIKEKDSE LNQKRPQYIK
AKENTSHKIK KLEAAKKSLQ HAQKHYKKRK GDMDELEKEM LSVEKARQEF EERMEEESQS
QGRDLTLEEN QVKKYHRLKE EASKRAATLA QELEKFNRDQ KADQDRLDLE ERKKVETEAK
IKQKLREIEE NQKRIEKLEE YITTSKQSLE EQKKLEGELT EEVEMAKRRI DEINKELNQV
MEQLGDARID RQESSRQQRK AEIMESIKRL YPGSVYGRLI DLCQPTQKKY QIAVTKVLGK
NMDAIIVDSE KTGRDCIQYI KEQRGEPETF LPLDYLEVKP TDEKLRELKG AKLVIDVIRY
EPPHIKKALQ YACGNALVCD NVEDARRIAF GGHQRHKTVA LDGTLFQKSG VISGGASDLK
AKARRWDEKA VDKLKEKKGR LTEELKEQMK AKRKEAELRQ VQSQAHGLQM RLKYSQSDLE
QTKTRHLALN LQEKSKLESE LANFGPRIND IKRIIQSRER EMKDLKEKMN QVEDEVFEEF
CREIGVRNIR EFEEEKVKRQ NEIAKKRLEF ENQKTRLGIQ LDFEKNQLKE DQDKVHMWEQ
TVKKDENEIE KLKKEEQRHM KIIDETMAQL QDLKNQHLAK KSEVNDKNHE MEEIRKKLGG
ANKEMTHLQK EVTAIETKLE QERSDRHNLL QACKMQDIKL PLSEGTMDDI SQEEGSSQGE
ESVSGSQRTS SIYAREALIE IDYGDLCEDL KDAQAEEEIK QEMNTLQQKL NERQSVLQRI
AAPNMKAMEK LESVRDKFQE TSDEFEAARK RAKKAKQAFE QIKKERFDRF NACFESVATN
IDEIYKALSR NSSAQAFLGP ENPEEPYLDG INYNCVAPGK RFRPMDNLSG GEKTVAALAL
LFAIHSYKPA PFFVLDEIDA ALDNTNIGKV ANYIKEQSTC NFQAIVISLK EEFYTKAESL
IGVYPEQGDC VISKVLTFDL TKYPDANPNP NEQ 1233

mSMCD

MYIKQVIIQG FRSYRDQTIV DPFSSKHNVI VGRNGSGKSN FFYAIQFVLS DEFSHLRPEQ
RLALLHEGTG PRVISAFVEI IFDNSDNRLP IDKEEVSLRR VIGAKKDQYF LDKKMVTKND
VMNLLESAGF SRSNPYYIVK QGKINQMATA PDSQRLKLLR EVAGTRVYDE RKEESISLMK
ETEGKREKIN ELLKYIEERL HTLEEEKEEL AQYQKWDKMR RALEYTIYNQ ELNETRAKLD
ELSAKRETSG EKSRQLRDAQ QDARDKMEDI ERQVRELKTK ISAMKEEKEQ LSAERQEQIK
QRTKLELKAK DLQDELAGNS EQRKRLLKER QKLLEKIEEK QKELAETEPK FNSVKEKEER
GIARLAQATQ ERTDLYAKQG RGSQFTSKEE RDKWIKKELK SLDQAINDKK RQIAAIHKDL
EDTEANKEKN LEQYNKLDQD LNEVKARVEE LDRKYYEVKN KKDELQSERN YLWREENAEQ
QALAAKREDL EKKQQLLRAA TGKAILNGID SINKVLEHFR RKGINQHVQN GYHGIVMNNF
ECEPAFYTCV EVTAGNRLFY HIVDSDEVST KILMEFNKMN LPGEVTFLPL NKLDVRDTAY
PETNDAIPMI SKLRYNPRFD KAFKHVFGKT LICRSMEVST QLARAFTMDC ITLEGDQVSH
RGALTGGYYD TRKSRLELQK DVRKAEEELG ELEAKLNENL RRNIERINNE IDQLMNQMQQ
IETQQRKFKA SRDSILSEMK MLKEKRQQSE KTFMPKQRSL QSLEASLHAM ESTRESLKAE
LGTDLLSQLS LEDQKRVDAL NDEIRQLQQE NRQLLNERIK LEGIITRVET YLNENLRKRL
DQVEQELNEL RETEGGTVLT ATTSELEAIN KRVKDTMARS EDLDNSIDKT EAGIKELQKS
MERWKNMEKE HMDAINHDTK ELEKMTNRQG MLLKKKEECM KKIRELGSLP QEAFEKYQTL
SLKQLFRKLE QCNTELKKYS HVNKKALDQF VNFSEQKEKL IKRQEELDRG YKSIMELMNV
LELRKYEAIQ LTFKQVSKNF SEVFQKLVPG GKATLVMKKG DVEGSQSQDE GEGSGESERG
SGSQSSVPSV DQFTGVGIRV SFTGKQGEMR EMQQLSGGQK SLVALALIFA IQKCDPAPFY
LFDEIDQALD AQHRKAVSDM IMELAVHAQF ITTTFRPELL ESADKFYGVK FRNKVSHIDV
ITAEMAKDFV EDDTTHG 1217

Fig. 1.

mSMCB and mSMCD protein sequences. (**A**) Protein sequence inferred from the *mSMCB* cDNA. GeneBank Accession No. AF047600. (**B**) Protein sequence encoded by *mSMCD* cDNA. GeneBank Accession No. AF047601. The amino-terminal ATP-binding region and carboxy-terminal DA-box are underlined.

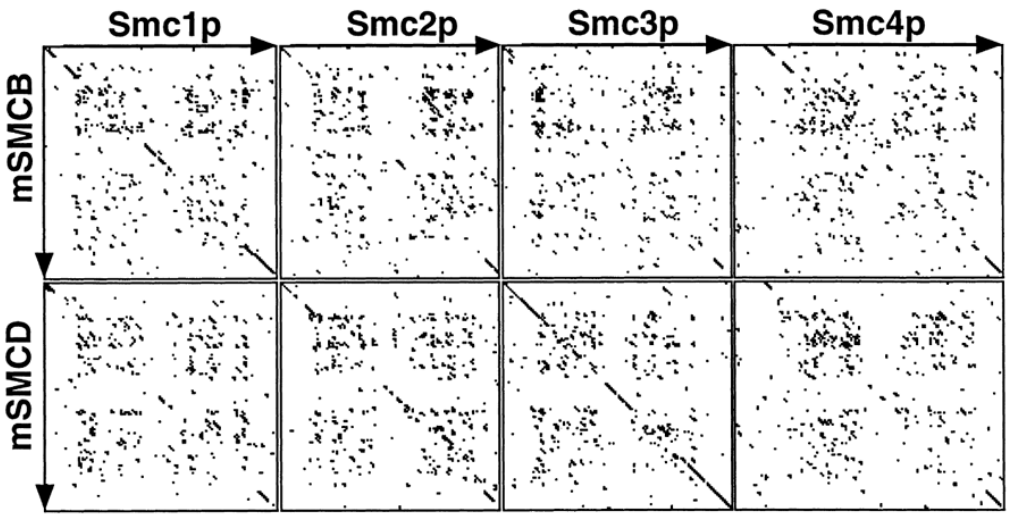

Fig. 2.

mSMCB and mSMCD protein sequence comparison to yeast SMC proteins. A dot matrix analysis was performed with a window of 23 and a stringency of 7.

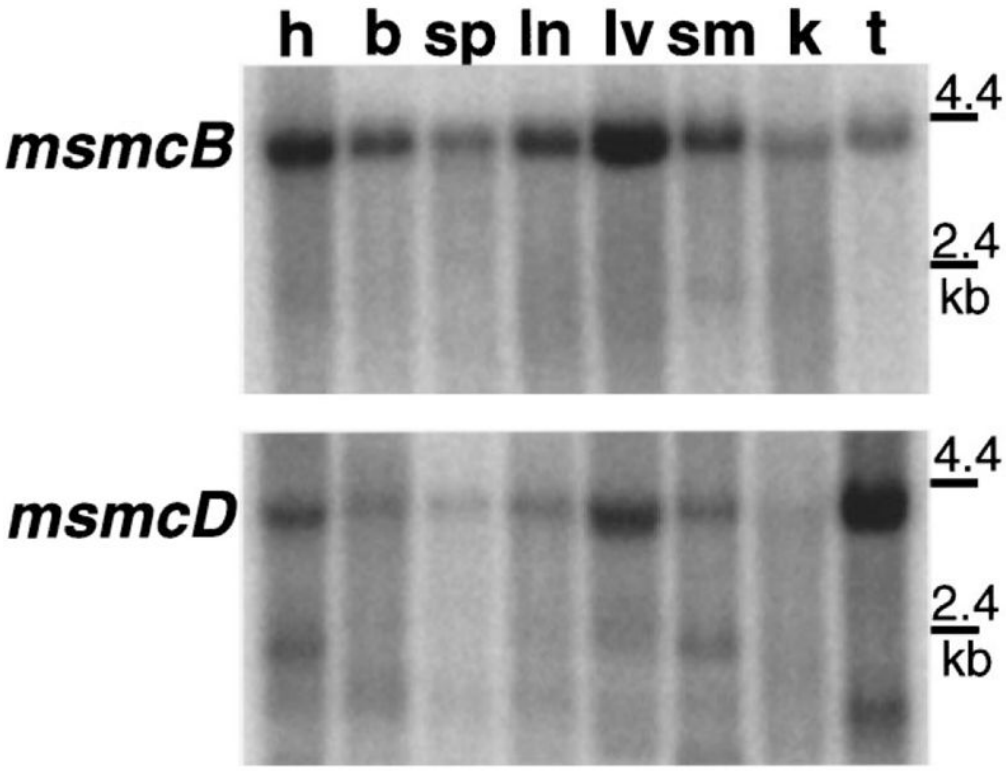

Fig. 3.

Characterization of mSMCB and mSMCD mRNA. (**A**) The mouse multiple tissue Multiple-tissue Northern blot (Clontech) was probed with internal probes derived from mSMCB and mSMCD cDNA. Two micrograms of poly-A RNA were loaded per lane. *h*, heart; *b*, brain; *sp*, spleen; *ln*, lung; *lv*, liver; *sm*, skeletal muscle; *k*, kidney; *t*, testis. A Northern hybridization using actin as a loading-control probe revealed a uniform loading in all lanes, except the skeletal muscle lane (data not shown).

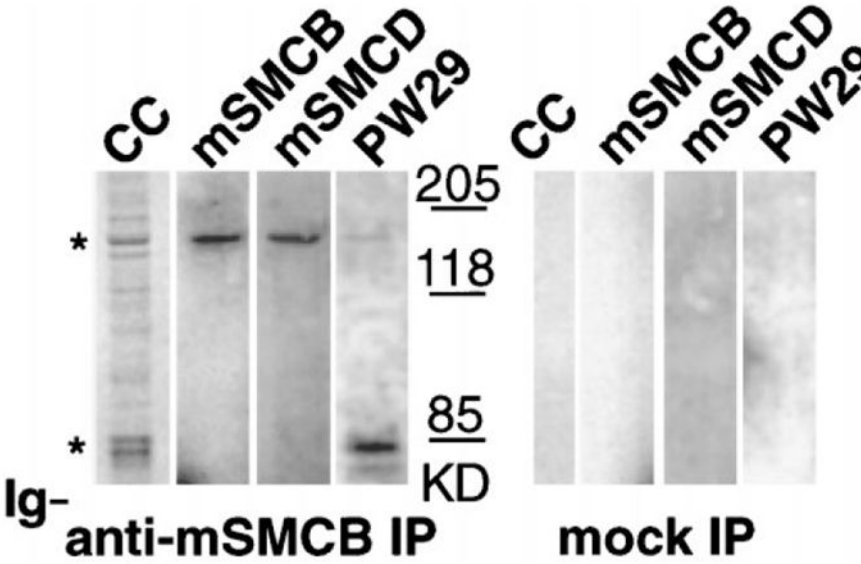

Fig. 4.

Coimmunoprecipitation of mSMCD and PW29 proteins with mSMCB. Immunoprecipitates from mouse embryonic extract (see Section 2) were separated on a NUPAGE Bis-Tris gel (Novex) and probed with affinity-purified anti-mSMCB (#2966, 1:500 dilution), affinity-purified anti-mSMCD (#3009, 1:250 dilution) and crude anti-PW29 (1:10 000 dilution) antibodies. Mock immunoprecipitations were performed under identical conditions, with precipitating antibody omitted.

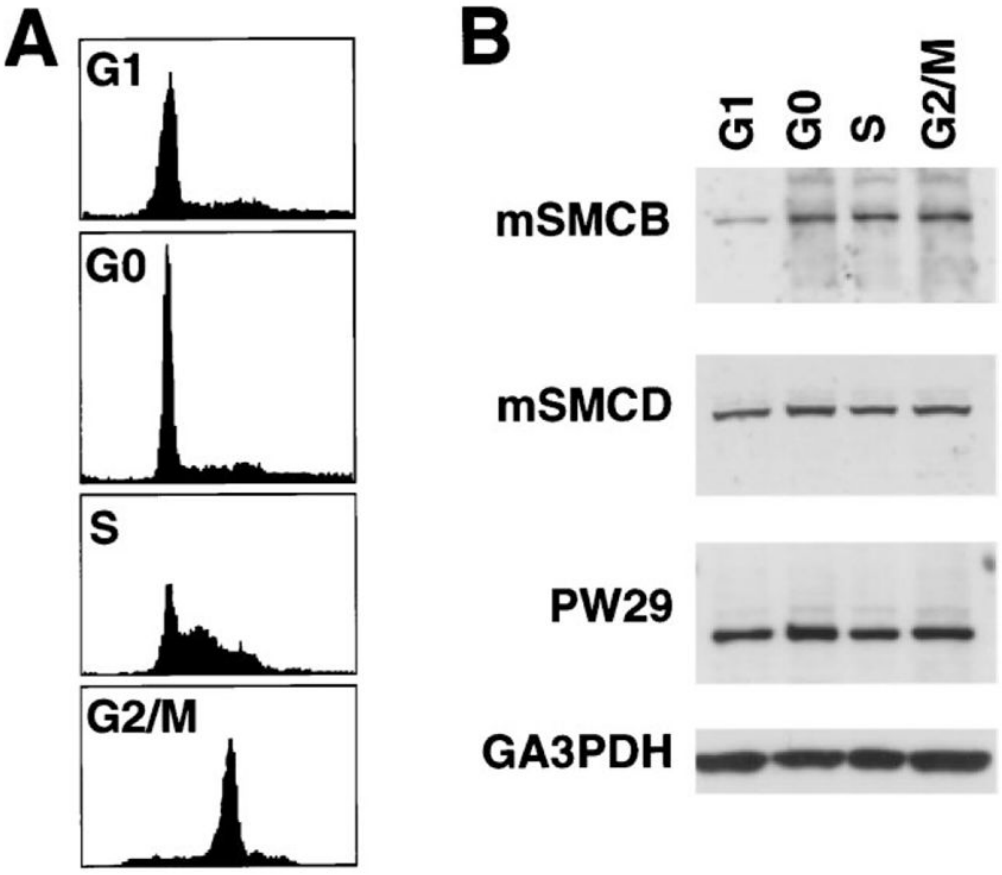

Fig. 5.

Cell-cycle expression pattern for mSMCB, mSMCD and PW29 proteins. (**A**) Characterization of the cell-cycle arrest in NIH3T3 cells by FACS analysis. Arresting factors: *G1*, lovastatin; *G0*, 0.5% serum starvation; *S*, aphidicolin; *G2*/*M*, nocodazole. (**B**) Comparison of intracellular levels of mSMCB, mSMCD and PW29 proteins at the arresting conditions corresponding to (**A**). Fifteen micrograms of protein were loaded per lane. GAP3DH levels are shown as a control for equal loading.

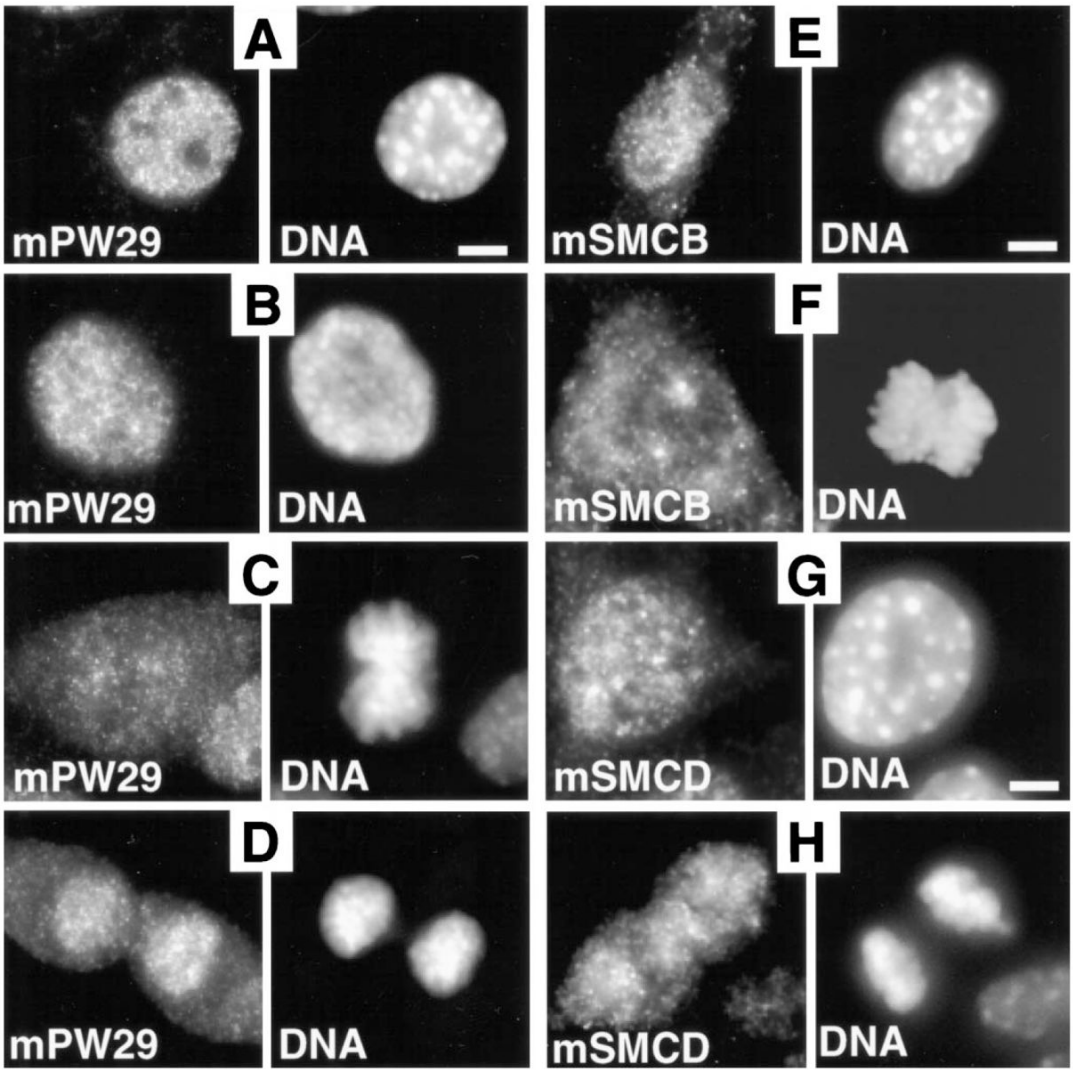

Fig. 6.

Localization of mouse mSMCB, mSMCD and PW29 proteins in asynchronously growing NIH3T3 cells. (**A**–**D**) Cells at different stages of the cell cycle, stained for PW29 with crude specific antiserum (1:10 000). Cells were also stained for DNA with DAPI and tubulin (not shown) with YOL1/34 antibody. (**E**) Interphase and (**F**) metaphase NIH3T3 cells stained with affinity-purified anti-mSMCB antibodies (1:2000) and DAPI. (**G**) Interphase and (**H**) anaphase NIH3T3 cells stained with affinity-purified anti-mSMCD antibodies (1:1000) and DAPI. Bars: 5 μm.

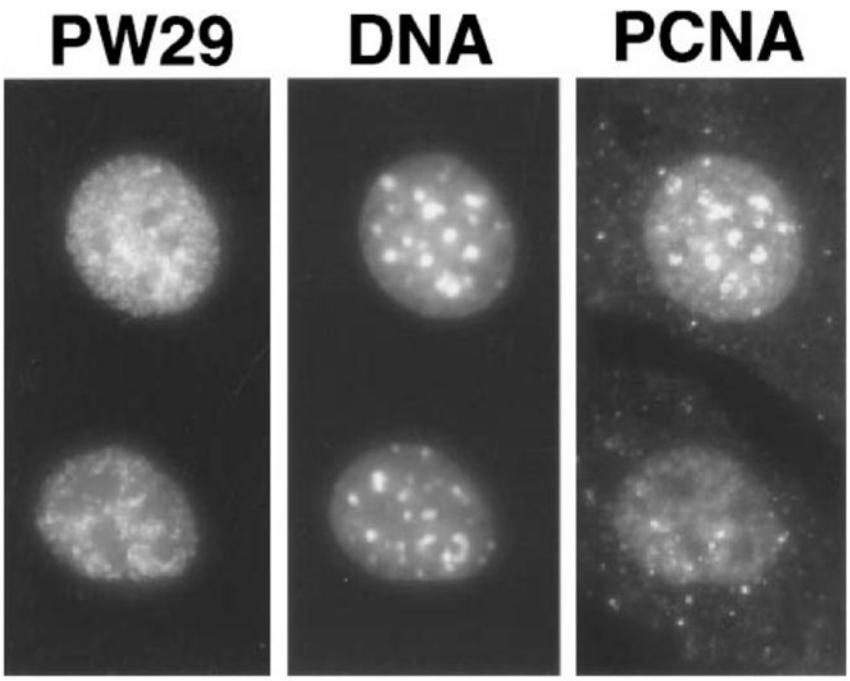

Fig. 7.

Localization of mouse PW29 protein and PCNA in asynchronously growing NIH3T3 cells. Two cells in the same field are at different stages of S-phase, based on staining for PCNA marker. PW29 localization (1:10 000 staining with crude serum) does not change with changed PCNA localization. Cells were also stained for DNA with DAPI and tubulin (not shown) with YOL1/34 antibody. Bar: 5 μm.